Contribution of Ballistic Electron Transport to Energy Transfer During Electron-Phonon Nonequilibrium in Thin Metal Films

Patrick E. Hopkins[1]

Pamela M. Norris[2]
e-mail: pamela@virginia.edu

Department of Mechanical and Aerospace Engineering,
University of Virginia,
Charlottesville, VA 22904-4746

With the ever decreasing characteristic lengths of nanomaterials, nonequilibrium electron-phonon scattering can be affected by additional scattering processes at the interface of two materials. Electron-interface scattering would lead to another path of energy flow for the high-energy electrons other than electron-phonon coupling in a single material. Traditionally, electron-phonon coupling in transport is analyzed with a diffusion (Fourier) based model, such as the two temperature model (TTM). However, in thin films with thicknesses less than the electron mean free path, ballistic electron transport could lead to electron-interface scattering, which is not taken into account in the TTM. The ballistic component of electron transport, leading to electron-interface scattering during ultrashort pulsed laser heating, is studied here by a ballistic-diffusive approximation of the Boltzmann transport equation. The results for electron-phonon equilibration times are compared with calculations with TTM based approximations and experimental data on Au thin films. [DOI: 10.1115/1.3072929]

Keywords: electron-phonon coupling, ultrashort pulsed laser heating, Boltzmann transport equation, ballistic-diffusive treatment, electron-interface scattering, thin films

1 Introduction

With the continued progress in development and production of nanostructures and nanosystems also comes development of high-powered high-precision measurement systems. Ultrashort pulsed laser systems are now commercially manufactured and marketed with optical pulses as short as a few femtoseconds. At these ultrashort time scales, ultrafast phenomena that are crucial in many nanoscale applications are directly observable, such as ablation and laser machining of materials [1–3], spin dynamics in magnetic materials [4–8], electron relaxation in metals [9–12], electron-phonon heat transfer in thin metal films [13–17], and electron-carrier processes in semiconductors [18,19]. These ultrafast phenomena often induce electron-phonon nonequilibrium, where the temperature of the free electron system can reach several thousands of Kelvin with just a few degrees of temperature increase in the lattice system. However, as engineers continue to fabricate materials and devices with decreasing characteristic lengths, the ultrafast processes become increasingly difficult to observe and characterize with femtosecond optical techniques due to the presence of material interfaces. For example, Hopkins and Norris [14] showed that electron-interface scattering affects transient thermoreflectance (TTR) [20] measurements of the electron-phonon coupling factor in thin Au films. They attributed this interference to ballistic electron transport resulting from the ultrashort femtosecond pulse leading to a thermal penetration depth of the electron system stretching to the Au film-substrate interface [13]. Therefore, during electron-phonon thermalization, the electron system also scatters at the Au/substrate interface and loses energy to the substrate, so the observed electron-phonon coupling factor is greater than that predicted via traditional models [21]. This suggests that during ultrashort pulsed laser heating, when the film thickness is less than the ballistic penetration depth of the electrons, there are two competing electron scattering processes affecting the equilibration of the "electron gas" with the surrounding media: electron-phonon scattering in the film due to diffusive electron transport and electron-interface scattering at the film/substrate interface due to ballistic electron transport.

In this report, the effects of ballistic electron transport after ultrashort pulsed laser heating are compared with the diffusive electron transport that contributes to electron-phonon coupling in thin metal films. Different effects of ballistic electron transport during electron-phonon nonequilibrium have been experimentally observed in Au by several groups [13,14,22,23], but the relative effects of ballistic and diffuse electron transport and subsequent scattering mechanisms have yet to be considered separately; this is possible by considering electron transport during electron-phonon nonequilibrium with the ballistic-diffusive approximation (BDA) [24,25] to the Boltzmann transport equation (BTE) [26].

2 Background

2.1 Two Temperature Model. Energy transport during electron-phonon nonequilibrium is described with the two temperature model (TTM) [27]. In thin metal films with thicknesses less than the thermal (ballistic) [13] penetration depths, δ, the TTM can be expressed in the simplified form that assumes the thermal gradient of the electron system is minimal [13,14], which, after short pulse absorption, is given by

$$C_e \frac{\partial T_e}{\partial t} = -G[T_e - T_L] \tag{1}$$

[1]Present address: Engineering Sciences Center, Sandia National Laboratories, P.O. Box 5800, Albuquerque, NM 87185-0346.

[2]Corresponding author.

Contributed by the Heat Transfer Division of ASME for publication in the JOURNAL OF HEAT TRANSFER. Manuscript received June 15, 2008; final manuscript received September 10, 2008; published online February 20, 2009. Review conducted by Robert D. Tzou. Paper presented at the 2008 International Conference on Micro/Nanoscale Heat Transfer (MNHT2008), Tainan, Taiwan, January 6–9, 2008.

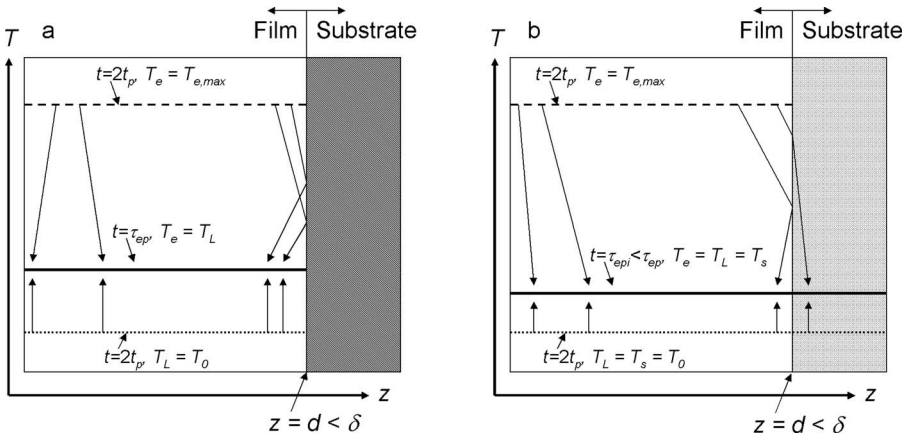

Fig. 1 Schematic of temperature changes of electron and lattice systems immediately after short-pulsed laser heating, in the case when the film thickness is less than the ballistic penetration depth. (*a*) Insulated boundary between the film and substrate: electron-phonon coupling will dominate the electron scattering events and drive electron cooling. Although electrons will traverse to the film/substrate interface, assuming an insulated boundary, the electrons will elastically reflect off the interface and travel back into the film and scatter with phonons in the film. (*b*) Uninsulated boundary between the film and substrate; electrons can inelastically scatter at the interface creating another form of energy loss from the electron system in addition to electron-phonon scattering in the film.

$$C_L \frac{\partial T_L}{\partial t} = G[T_e - T_L] \tag{2}$$

where C_e is the electron system heat capacity, T_e is the temperature of the electron system, G the electron-phonon coupling factor, C_L is the lattice heat capacity, and T_L the temperature of the lattice. Equation (1) is subject to $T_e(t=0)=T_{e,\max}$ and Eq. (2) is subject to $T_L(t=0)=T_0$, where $T_{e,\max}$ is the maximum electron temperature after laser absorption and T_0 is the initial temperature of the thin metal film. A schematic illustrating the change in electron and phonon temperatures at various times after pulse absorption (represented by $t=0$) up to the electron-phonon thermalization time, τ_{ep}, of the thermal processes described by Eqs. (1) and (2) are shown in Fig. 1(*a*). The scattering processes and temperature changes driving electron-phonon thermalization are illustrated by the arrows in this figure. In this thermal process, since the film-substrate boundary is considered "insulative" (i.e., any electron scattering occurring at the boundary is completely elastic and reflective) and since the ballistic penetration depth is greater than the film thickness, the thermal gradient in the electron system is considered negligible, and volumetric electron-phonon coupling is the primary mode of electron thermalization with the surrounding medium (being the film's lattice). Since $d<\delta$, there will be electron-interface scattering, but as previously mentioned, electrons elastically reflect off the interface then penetrate back into the film and scattering with phonons. In addition, note that the arrows representing the electron scattering processes are drawn slightly skewed from the vertical. This represents the fact that, although there is no net thermal gradient in the electron system, electrons still travel in all directions with different velocities (the net of which is zero), resulting in electron-phonon scattering. Also, since the ballistic penetration depth (which is related to the elastic electron mean free path, since multiple electron scattering events will give rise to electron relaxation into a Fermi distribution) is a statistical quantity, not all electrons will penetrate to a depth δ before electron-phonon scattering. This is depicted by the arrows in Fig. 1(*a*) that are not "reflecting" at the interface.

The electron cooling process in Fig. 1(*a*), which is mathematically explained by the TTM, describes energy exchange between a hot electron system and a colder lattice system via electron-phonon scattering events with the electron-phonon coupling factor, which is a function of the electron-phonon relaxation time [28]. These scattering events make this thermal process diffusive by nature, and the TTM can be derived from the BTE under the relaxation time approximation using the electron-phonon relaxation time as the time it takes for the electron system to return to an equilibrium Fermi distribution [29]. However, the ballistic transport that occurs in the electron system, immediately after pulsed laser heating [13,22], can influence the electron scattering dynamics and energy transfer in thin films with thicknesses less than the ballistic penetration depth due to inelastic electron-interface scattering at the film/substrate interface [14]. Evidence of this inelastic electron-interface scattering affecting electron cooling has been shown even in thermally insulative substrates [14]. In this case, inelastic electron scattering at the film/substrate interface would cause energy loss from the film electron system and increase the electron-phonon thermalization time, since the electrons could loose energy to (1) the substrate via electrons traveling ballistically and inelastically scattering at the interface and (2) the film lattice via electrons traveling diffusely and scattering with phonons. When considering inelastic electron-interface scattering (and neglecting phonon-interface scattering typically associated with phonon thermal boundary resistance [30]), the electron-phonon-interface thermalization time, τ_{epi}, would be driven by the scattering processes and temperature changes illustrated by the arrows in Fig. 1(*b*), which depicts electrons inelastically scattering at the interface and transferring energy away from the film media. Note that Fig. 1(*b*) depicts the final temperature of the film to be less than that depicted in Fig. 1(*a*) due to the inelastic electron-interface scattering events transferring more film electron energy away from the film into the substrate.

Although the thermal effects of the ballistic electron-interface scattering have been indirectly studied with a three temperature model (3TM) [14], the 3TM approach still assumes complete diffusive transport. Therefore, the explicit contribution of ballistic electron transport and subsequent scattering processes on electron system relaxation other than electron-phonon scattering (such as inelastic electron-interface scattering at a film-substrate interface) cannot be studied with these diffusive treatments.

2.2 Ballistic-Diffusive Approximations for the BTE. Studying the ballistic nature of electron transport during electron-phonon nonequilibrium must start with the BTE for electrons [29], given by

$$\frac{\partial f}{\partial t} + \boldsymbol{v}\nabla_{\boldsymbol{r}} f + \frac{e}{m}\boldsymbol{E}\cdot\nabla_{\boldsymbol{v}} f = \left(\frac{\partial f}{\partial t}\right)_c \tag{3}$$

where f is the nonequilibrium electron distribution, $\boldsymbol{v}$ the velocity vector, $\boldsymbol{r}$ the position vector, e the electric charge, m the mass of an electron, $\boldsymbol{E}$ the electric field, the quantity $e\boldsymbol{E}$ the Lorentz force resulting from the electric field, and the term $(\partial f/\partial t)_c$ the time rate of change of the nonequilibrium electron distribution due to electron collisions. Assuming one-dimensional (1D) heat flow, which is often assumed in ultrashort pulsed laser heating analyses [28,31], Eq. (3) becomes

$$\frac{\partial f}{\partial t} + v_z\frac{\partial f}{\partial z} + \frac{F_z}{m}\frac{\partial f}{\partial v_z} = \left(\frac{\partial f}{\partial t}\right)_c \tag{4}$$

where z is the direction perpendicular to the film surface, and F_z represents the Lorentz force. As previously mentioned, estimating the collision term of Eq. (4) with the relaxation time approximation and taking the relaxation time as the electron-phonon thermalization time leads to the traditional TTM [27], as outlined by Chen et al. [29].

However, in the event of ultrashort pulsed laser absorption by the electron system and subsequent ballistic penetration to a depth greater than the film thicknesses, the electrons traveling ballistically can scatter at the film/substrate interface and significantly change the electron relaxation dynamics [14]. In order to understand the relative contributions of the ballistic electron-interface scattering and the diffusive electron-phonon scattering, the BDA must be employed to the BTE [24,25]. The BDA separates the intensity of energy carriers, I, at any point into two parts: the ballistic intensity, I_b, which represents carriers originating from the boundaries and experiencing out-scattering only, and the diffusive intensity, I_m, which represents carriers originating from inside the medium due to the excitation and the boundary contribution converted into scattered or emitted carriers after absorption. This solution technique has been used to study phonon transport and ballistic phonon scattering under a single relaxation time approximation [24,25,32], transforming the distribution function notation of the BTE into intensity notation [33]. In this work, in the limiting case of $d < \delta$ and assuming no thermal gradient, the BTE for electrons will be used to calculate the ballistic and diffusive electron intensities and to compare the relative contributions of inelastic interface scattering from ballistic transport and phonon scattering from diffusive transport to electron-media thermalization.

3 Separation of Ballistic and Diffusive Electron Scattering

3.1 The Equation of Electron Energy Transfer. The 1D BTE for electrons is given by Eq. (4). When $d < \delta$, no thermal gradient exists in the electron system, and therefore Eq. (4) becomes

$$\frac{\partial f}{\partial t} = \left(\frac{\partial f}{\partial t}\right)_c \tag{5}$$

Paralleling the equation of phonon radiative transport (EPRT) [33], the equation of electron energy transfer (EEET) is established by multiplying each term in Eq. (5) by the product $\varepsilon D(\varepsilon)$, where ε is the electron energy and $D(\varepsilon)$ is the electron density of states yielding

$$\frac{\partial U}{\partial t} = \left(\frac{\partial U}{\partial t}\right)_c \tag{6}$$

where U is the volumetric electron energy density, defined as $U = \varepsilon D(\varepsilon) f$, and Eq. (6) is subject to the following initial condition:

$$U(0) = S = \frac{(1-R)J}{d} \tag{7}$$

In this case, the initial condition S is the energy absorbed by electrons per unit volume. This is related to $T_{e,\max}$ in Eq. (1) by $\int_{T_0}^{T_{\max}} C_e(T_e)dT = S$. The source term assumes that the incident energy is absorbed instantaneously and homogeneously throughout the depth of the film (the energy is actually absorbed in the optical penetration depth, but then stretched out into the film thickness by electrons traveling ballistically if $d < \delta$). Applying the relaxation time approximation [26] to the EEET yields

$$\frac{\partial U}{\partial t} = -\frac{U - U_0}{\tau} \tag{8}$$

where U_0 is the equilibrium electron energy density per unit energy in the film defined as $U_0 = \int_\varepsilon \varepsilon D(\varepsilon) f_0 d\varepsilon$, where f_0 is the Fermi–Dirac distribution function. Here, τ is the relaxation time of the electrons in the metal films, which for purely diffusive transport (i.e., a completely insulative substrate, as discussed with respect to Fig. 1(*a*)) and for the temperatures and time scales of interest is the electron-phonon thermalization time, τ_{ep}.

In this work, only electron temperatures less than 4000 K will be considered to directly compare with pump probe experimental data on Au [14]. Therefore, this analysis will focus on free electron (noble) metals, and this temperature range ensures the following:

(1) a linear heat capacity [34] so $C_e(T_e) = \gamma T_e$ and therefore the maximum electron temperature after pulse absorption can be estimated by $T_{e,\max} = \sqrt{2S/\gamma + T_0^2}$
(2) a relatively constant chemical potential, μ, that is approximately equal to the Fermi energy, ε_F [34]
(3) a relatively constant electron-phonon coupling factor in the free electron metal [21,34]
(4) an electron spectral energy range participating in thermal processes within $\varepsilon \pm k_B T_e$, where k_B is the Boltzmann constant [35]
(5) an unmodified lattice from the incident laser pulse (i.e., no ablation or spallation [1])
(6) a parabolic conduction band leading to a conduction electron density of states per unit energy given by $D(\varepsilon) = (3n/2)(\varepsilon/\varepsilon_F)^{1/2}(1/\varepsilon_F)$ [35], where n is the conduction electron number density (a derivation of this less-often-used form of the density of states is given in the Appendix)

3.2 Complete Elastic Electron Interface Scattering (i.e., No Electron Energy Loss to the Substrate). Applying the BDA to electron transport after short-pulsed laser heating uses a slightly different approach than previous works applying the BDA to phonon transport [24,25,32]—specifically the single relaxation time approximation. Electron-phonon nonequilibrium resulting from pulsed laser heating can be divided into two characteristic time intervals [13,36]. The earliest of the time intervals, the duration of which is termed the electron-electron relaxation time, τ_{ee}, is typically on the order of 10–100 fs for metals [31]. This time represents the time it takes for the excited electrons to relax into a Fermi distribution through *e-e* (electron-electron) collisions, which dominate *e-p* (electron-phonon) collisions during this time interval. Ballistic transport of the electrons occurs over this time. Once equilibrium is achieved within the electron system, the higher temperature electrons transmit energy to the lattice through *e-p* scattering processes over the electron-phonon relaxation time (often referred to as the electron-phonon thermalization time), τ_{ep}.

The heat transferred via these *e-p* interactions is governed by Eqs. (1) and (2). Thermalization time is typically on the order of 1 ps for metals and is inversely related to the electron-phonon coupling factor [28]. Due to the differing relaxation times governing ballistic and diffusive (electron-phonon) transport processes, ballistic electron transport must be modeled with τ_{ee} and diffusive electron transport must be modeled with τ_{ep}.

Therefore, to separate ballistic and diffusive electron transport, the EEET (Eq. (6)) can be rewritten as

$$\frac{\partial U}{\partial t} = \frac{\partial}{\partial t}(U_b + U_m) = \left(\frac{\partial U_b}{\partial t}\right)_c + \left(\frac{\partial U_m}{\partial t}\right)_c \tag{9}$$

or by applying the relaxation time approximation

$$\frac{\partial U}{\partial t} = \frac{\partial}{\partial t}(U_b + U_m) = -\frac{U_b - U_m}{\tau_{ee}} - \frac{U_m - U_0}{\tau_{ep}} \tag{10}$$

Note in Eq. (10), since $\tau_{ee} < \tau_{ep}$, the ballistic component relaxes to the diffusive component over τ_{ee}, which in turn relaxes to the equilibrium distribution over τ_{ep}. Also, Eq. (8) can in fact be approximated with a single relaxation time approximation, following previous BDAs relating to phonon transport with the stipulation that $U_b=0$ when $t > \tau_{ee}$. Relating the ballistic and diffusive terms, and recognizing that S is absorbed by the ballistically traveling electrons, yields

$$\frac{\partial U_b}{\partial t} = -\frac{U_b - U_m}{\tau_{ee}} \tag{11}$$

and

$$\frac{\partial U_m}{\partial t} = -\frac{U_m - U_0}{\tau_{ep}} \tag{12}$$

where Eqs. (11) and (12) are subject to

$$U_b(0) = S \tag{13}$$

and

$$U_m(0) = U_b(\tau_{ee}) \tag{14}$$

respectively. Technically, there is a time delay in the development of the diffusively scattering electron system since the ballistic system relaxes to the diffusive system, and therefore Eq. (14) should read $U_m(\tau_{ee}) = U_b(\tau_{ee})$. However, this work is not focused on *when* the energy is transferred but *how* the energy is transferred, and therefore for ease of calculation and discussion, the diffusive component to the electron energy is prescribed to begin at $t=0$. Therefore, by imposing Eq. (14) as an initial condition, Eq. (12) is rewritten as

$$\frac{\partial U_m}{\partial t} = -\frac{U_m - U_0}{\tau_{ep} - \tau_{ee}} \tag{15}$$

The solution of the ballistic component is given by

$$U_b(t) = U_m\left(1 - \exp\left[-\frac{t}{\tau_{ee}}\right]\right) + S\exp\left[-\frac{t}{\tau_{ee}}\right] \tag{16}$$

and the diffusive component is given by

$$U_m(t) = \frac{U_0\left(1 - \exp\left[-\dfrac{t}{\tau_{ep} - \tau_{ee}}\right]\right) + S\exp\left[-\dfrac{t}{\tau_{ep} - \tau_{ee}} - 1\right]}{1 - \exp\left[-\dfrac{t}{\tau_{ep} - \tau_{ee}}\right] + \exp\left[-\dfrac{t}{\tau_{ep} - \tau_{ee}} - 1\right]} \tag{17}$$

Equations (11) and (15) subject to Eqs. (13) and (14) represent the "BDA" of the EEET for the electron system excited by an ultrashort laser pulse in which ($d < \delta$) and elastic electron-interface scattering occurs (shown in Fig. 1(*a*)). The solutions are given by Eqs. (16) and (17). The average energy densities over the thermalization times of the ballistic and diffusive components are given by

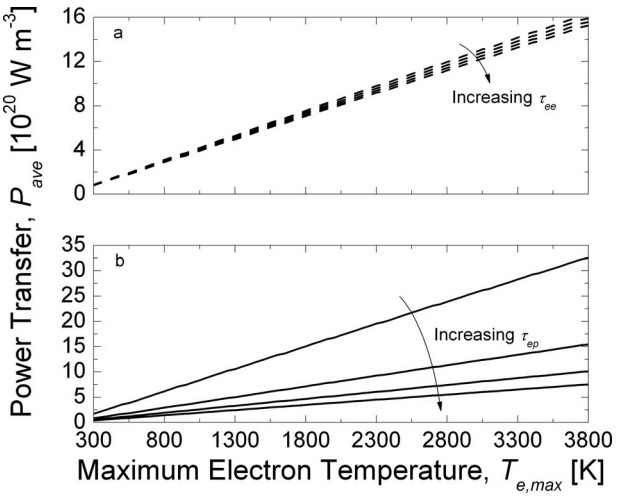

Fig. 2 Average power density transferred from the electron system assuming no energy loss to the substrate (elastic electron-interface scattering) as a function of maximum electron temperature in the (*a*) ballistic regime assuming τ_{ee} of 50 fs, 200 fs, 350 fs, and 500 fs and τ_{ep} of 4 ps (Eq. (20)) and (*b*) diffusive regime (electron-phonon coupling) assuming τ_{ee} of 200 fs and τ_{ep} of 2 ps, 4 ps, 6 ps, and 8 ps (Eq. (21)).

$$U_{b,\mathrm{avg}} = \frac{1}{\tau_{ee}}\int_0^{\tau_{ee}} U_b(t)dt \tag{18}$$

and

$$U_{m,\mathrm{avg}} = \frac{1}{\tau_{ep} - \tau_{ee}}\int_0^{\tau_{ep}-\tau_{ee}} U_m(t)dt \tag{19}$$

Therefore, the average power density transferred from the ballistic and diffusive electron systems over each system's respective thermalization time is given by

$$P_{b,\mathrm{avg}} = \frac{U_{b,\mathrm{avg}}}{\tau_{ee}} \tag{20}$$

$$P_{m,\mathrm{avg}} = \frac{U_{m,\mathrm{avg}}}{\tau_{ep} - \tau_{ee}} \tag{21}$$

Figures 2(*a*) and 2(*b*) show the power density transferred from the ballistic and diffusive electron system in a Au film over their respective thermalization times as a function of maximum electron temperature assuming $S = (\gamma(T_{e,\max}^2 - T_0^2))/2$. These calculations assume elastic electron-interface scattering, and therefore all the energy from S remains in the electron system during the ballistic transport regime. For Au, $\gamma = 71.4$ J m^{-3} K^{-2}, $\varepsilon_F = 5.53$ eV, and $n = 5.9 \times 10^{28}$ m^{-3} [37]. Figure 2(*a*) shows ballistic power density calculations assuming a constant τ_{ep} of 4 ps with various τ_{ee}'s (50 fs, 200 fs, 350 fs, and 500 fs). Figure 2(*b*) shows diffusive power density calculations assuming a constant τ_{ee} of 200 fs with various τ_{ep}'s (2 ps, 4 ps, 6 ps, and 8 ps). The electron-electron relaxation times were chosen since τ_{ee} in Au has been theoretically calculated to be as low as about 50 fs [31] and experimentally measured to be as large as 500 fs [12]. The power density of the ballistic contribution weakly depends on electron-electron thermalization time, where the diffusive contribution is strongly dependent on thermalization time. This diffusive electron

power density dependency on electron-phonon thermalization time is expected since the electron-phonon coupling factor is inversely related to τ_{ep} via $G=\gamma T_e/\tau_{ep}$ [38].

The electron-phonon coupling factor in metals has been extensively studied, and the temperature functionality of G has been well studied numerically [21,34,39]. In the case of Au in the temperature range of interest in this work, G is a constant value of about 2.4×10^{16} W m^{-3} K^{-1}, which has been verified experimentally [13,16,40,41]. Since G represents the diffusive electron-phonon scattering in this work, the power transferred by the electron system by diffusive scattering events (Eq. (21)) can be recast into terms of G as

$$P_{m,\mathrm{avg}}=\frac{1}{\left(\frac{\gamma T_{e,\max}}{G}-\tau_{ei}\right)^2}\int_0^{\gamma T_{e,\max}/G-\tau_{ee}}\left(\int_{\varepsilon_F-k_B}^{\varepsilon_F+k_B}\varepsilon D(\varepsilon)f_0 d\varepsilon\frac{\left(1-\exp\left[-\frac{t}{\frac{\gamma T_{e,\max}}{G}-\tau_{ee}}\right]\right)+S\exp\left[-\frac{t}{\frac{\gamma T_{e,\max}}{G}-\tau_{ee}}-1\right]}{1-\exp\left[-\frac{t}{\frac{\gamma T_{e,\max}}{G}-\tau_{ee}}\right]+\exp\left[-\frac{t}{\frac{\gamma T_{e,\max}}{G}-\tau_{ee}}-1\right]}\right)dt \quad (22)$$

where Eq. (22) takes into account a change in electron-phonon thermalization time based on the maximum electron temperature achieved after laser heating through $\tau_{ep}=\gamma T_{e,\max}/G$. This assumption keeps calculations in line with the definition of the laser source term, S. Figure 3 shows the ratio of the ballistic power density to the diffusive power density as a function of electron temperature using Eqs. (20) and (22). Figure 3 shows calculations of $P_{b,\mathrm{avg}}/P_{m,\mathrm{avg}}$ for four different τ_{ee}'s (50 fs, 200 fs, 350 fs, and 500 fs). The calculations show that, for this case of elastic electron-interface scattering leading to electron-electron then electron-phonon thermalization, the power transferred from the electrons traveling ballistically is approximately equal to the power transferred from the thermalized electron system to the phonons during electron-phonon thermalization at high electron temperatures. At relatively low electron temperatures (close to room temperature) the power transferred during ballistic processes is less than that during diffusive electron-phonon processes.

3.3 Inelastic Electron Interface Scattering (i.e., Electron Energy Loss to the Substrate). Technically, since Eq. (11) represents the ballistic carriers scattering among themselves to relax into a thermal distribution, the term BDA is used loosely. Although the ballistic and diffusive components to electron transport are separated, they are effectively separated by considering two different EEETs: one for the electron-electron relaxation and one for the electron-phonon relaxation. However, in the case of inelastic electron-interface scattering, the ballistic carriers that inelastically scatter at the film/substrate interface experience no internal scattering. The energy of these carriers originates from the pulse absorption from the surface. In this case, the BDA of the EEET takes a slightly different form, more in line with the original BDA of the EPRT developed by Chen [24,25].

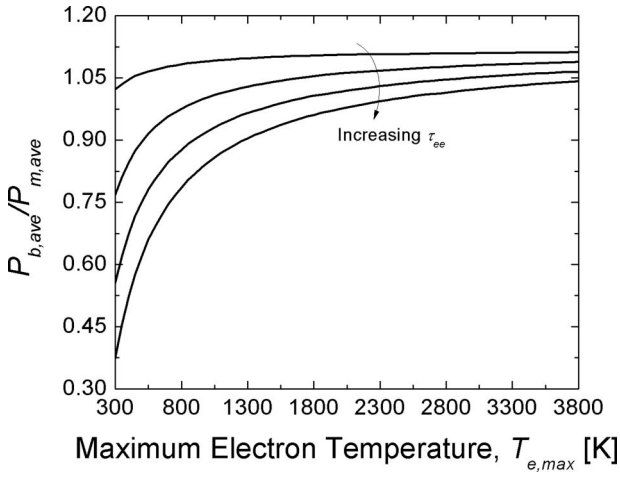

Fig. 3 Ratio of average power density transferred from ballistic processes to diffusive processes (ratio of Eq. (20) to Eq. (22)) as a function of maximum electron temperature. These calculations assume a temperature dependent electron-phonon relaxation time of $\tau_{ep}=\gamma T_{e,\max}/G$ and no energy loss to the substrate. Calculations shown assume τ_{ee} of 50 fs, 200 fs, 350 fs, and 500 fs.

As with the purely elastic scattering case, the ballistically and diffusively traveling electrons are considered as two separate systems, but to consider inelastic electron energy loss to the substrate as a result of electron-interface scattering, a new relaxation time, the electron-interface relaxation time, τ_{ei}, is applied to the ballistic system. If electrons elastically reflect off the interface, then they will eventually thermalize and scatter with phonons. Since the goal of this work is to compare the effects of inelastic interface scattering from ballistic electron transport to electron-phonon thermalization from diffusive electron transport, the elastically reflected electrons can be lumped in with the diffusive electron-phonon relaxation term. With this in mind, Eq. (6) can be rewritten as

$$\frac{\partial U}{\partial t}=\frac{\partial}{\partial t}(U_{bi}+U_m)=-\frac{U_{bi}}{\tau_{ei}}-\frac{U_m-U_0}{\tau_{ep}-\tau_{ee}} \quad (23)$$

where the subscript "*bi*" refers to the ballistic component inelastically scattering at the interface. Note that the inelastically interfacially scattered electrons do not relax to any particular energy since the energy of these electrons leave the film system; they experience out-scattering only as prescribed for the ballistic carriers in the original BDA development [24,25]. Again, the ballistic and diffusive terms on each side of Eq. (23) can be related yielding

$$\frac{\partial U_{\mathrm{bi}}}{\partial t}=-\frac{U_{\mathrm{bi}}}{\tau_{ei}} \quad (24)$$

and

$$\frac{\partial U_m}{\partial t}=-\frac{U_m-U_0}{\tau_{ep}-\tau_{ee}} \quad (25)$$

subject to

$$U_{\mathrm{bi}}(0)=S \quad (26)$$

and

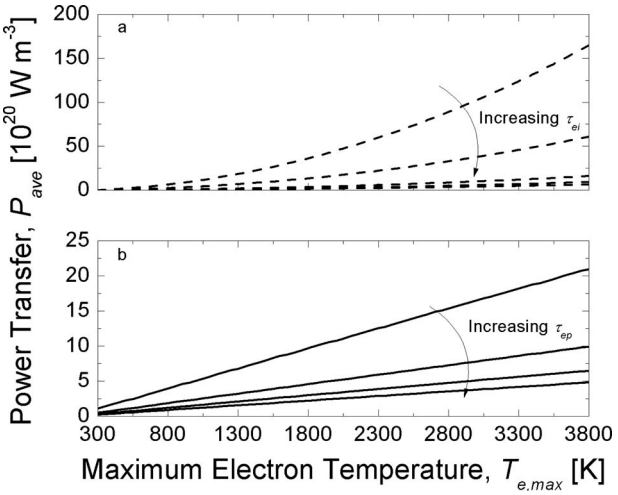

Fig. 4 Average power density transferred from the electron system assuming energy loss to the substrate (inelastic electron-interface scattering) as a function of maximum electron temperature in the (*a*) ballistic regime assuming τ_{ei} of 15 fs, 50 fs, 200 fs, 350 fs, and 500 fs and τ_{ep} of 4 ps (Eq. (30)) and (*b*) diffusive regime (electron-phonon coupling) assuming τ_{ee} of 200 fs and τ_{ep} of 2 ps, 4 ps, 6 ps, and 8 ps (Eq. (31)).

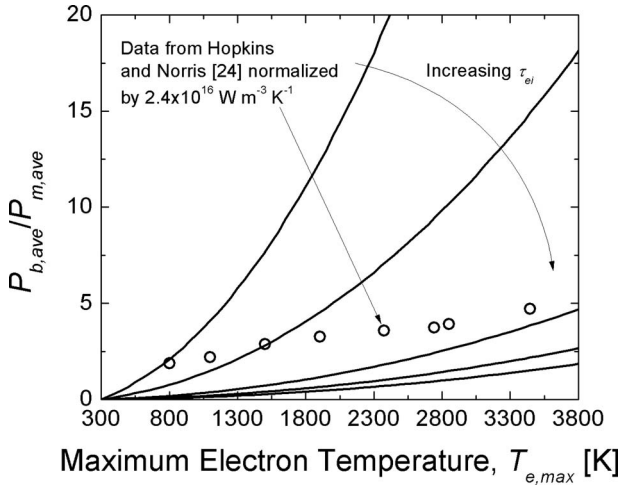

Fig. 5 Ratio of average power density transferred from ballistic processes to diffusive processes (ratio of Eq. (30) to Eq. (32)) as a function of maximum electron temperature. These calculations assume a temperature dependent electron-phonon relaxation time of $\tau_{ep}=\gamma T_{e,\max}/G$ and energy loss to the substrate from inelastic electron-interface scattering events during electron-electron thermalization. Calculations shown assume τ_{ei} of 15 fs, 50 fs, 200 fs, 350 fs, and 500 fs. Also shown in the figure are experimental pump probe *G*s measured on 20 nm Au films on Si substrates as a function of maximum electron temperature as measured by Hopkins and Norris [14]. Their data are normalized by the accepted value of *G* in Au, $G=2.4\times10^{16}$ W m^{-3} K^{-1}. The experimental work from Hopkins and Norris concluded that electron-interface scattering could increase the rate of electron-phonon equilibration in the film by providing another channel of energy transfer. This same conclusion is apparent in the calculations shown in this figure.

$$U_m(0) = S - U_{\rm bi}(\tau_{ei}) \tag{27}$$

Again, Eq. (25) assumes that $t=0$ is the time when the electron system in the film has reached a thermal Fermi distribution. These equations also assume that $\tau_{ei} < \tau_{ee}$, which is valid since the flight time of an electron in a thin film during Fermi relaxation is on the order to $t_{\rm flight}=d/v_F$, where v_F is the Fermi velocity. The solutions to Eqs. (24) and (25) are given by

$$U_{bi}(t) = S\exp\left[-\frac{t}{\tau_{ei}}\right] \tag{28}$$

and

$$U_m(t) = U_0\left(1-\exp\left[-\frac{t}{\tau_{ep}-\tau_{ei}}\right]\right) + S\left(\exp\left[-\frac{t}{\tau_{ep}-\tau_{ei}}\right]-\exp\left[-\frac{t}{\tau_{ep}-\tau_{ei}}-1\right]\right) \tag{29}$$

The average energy densities of the ballistic and diffusive components are calculated with equations analogous to Eqs. (18) and (19). Therefore, following Eqs. (20) and (21), the power densities transferred during scattering in ballistic and diffusive transport assuming inelastic electron-interface scattering are given by

$$P_{bi,\rm avg}=\frac{1}{\tau_{ei}^2}\int_0^{\tau_{ei}} S\exp\left[-\frac{t}{\tau_{ei}}\right]dt \tag{30}$$

and

$$P_{m,\rm avg}=\frac{1}{(\tau_{ep}-\tau_{ei})^2}\times\int_0^{\tau_{ep}-\tau_{ee}}\left(\left\{\int_{\varepsilon_F-k_B}^{\varepsilon_F+k_B}\varepsilon D(\varepsilon)f_0 d\varepsilon\left(1-\exp\left[-\frac{t}{\tau_{ep}-\tau_{ei}}\right]\right)\right\} + S\left(\exp\left[-\frac{t}{\tau_{ep}-\tau_{ei}}\right]-\exp\left[-\frac{t}{\tau_{ep}-\tau_{ei}}-1\right]\right)\right)dt \tag{31}$$

Figures 4(*a*) and 4(*b*) show the power density transferred from the electron system due to ballistic-inelastic interface scattering and diffusive electron-phonon scattering in a Au film over their respective thermalization times using Eqs. (30) and (31). These calculations use the same parameters as the calculations shown in Figs. 2(*a*) and 2(*b*), only this time including an electron-interface relaxation time of 15 fs to simulate the time-of-flight of an electron in a Au lattice traversing across a 20 nm film ($t_{\rm flight}=d/v_F$ $=20$ nm$/(1.4\times10^6$ m s$^{-1})\approx15$ fs). A similar trend is seen with the diffusive component as compared with that in Fig. 2(*b*). However, the ballistic power transfer is much larger in this case of inelastic electron-interface scattering and electron system energy loss compared with no electron system energy loss as modeled in Fig. 2(*a*), especially at high temperatures and low electron-interface relaxation times.

Following Eq. (22), Eq. (31) can be recast in terms of G as

$$P_{m,\rm avg}=\frac{1}{\left(\frac{\gamma T_{e,\max}}{G}-\tau_{ei}\right)^2}\times\int_0^{\gamma T_e/G-\tau_{ee}}\left(\left\{\int_{\varepsilon_F-k_B}^{\varepsilon_F+k_B}\varepsilon D(\varepsilon)f_0 d\varepsilon\left(1-\exp\left[-\frac{t}{\frac{\gamma T_{e,\max}}{G}-\tau_{ei}}\right]\right)\right\} + S\left(\exp\left[-\frac{t}{\frac{\gamma T_{e,\max}}{G}-\tau_{ei}}\right]-\exp\left[-\frac{t}{\frac{\gamma T_{e,\max}}{G}-\tau_{ei}}-1\right]\right)\right)dt \tag{32}$$

Figure 5 shows the ratio of ballistic to diffusive power densities (ratio of Eq. (30) to Eq. (32)) for the five different electron-

interface relaxation times shown in Fig. 4(*a*). These calculations assume that energy is being lost from the electron system in the film due to inelastic electron-interface scattering. The results show that the power transferred from the electron system through ballistic electron scattering can be much greater than the power transferred via diffusive electron scattering at high electron temperatures (4000 K) and low thermalization times.

These results agree well with the trends seen in electron-phonon coupling measurements in 20 nm Au films on Si substrates as measured by Hopkins and Norris [14]. At low electron temperatures (low incident fluence), they measured G of 2.3×10^{16} W m^{-3} K^{-1}. At high electron temperatures (3500 K), they measured G of 11.23×10^{16} W m^{-3} K^{-1}. They attributed this increase to electron-interface scattering due to the large ballistic penetration depth in Au. The measured Gs by Hopkins and Norris divided by the theoretically accepted value of G (2.4×10^{16} W m^{-3} K^{-1}) as a function of maximum electron temperature are also shown in Fig. 5. The agreement between the data and the calculations in this paper suggest that inelastic electron-interface scattering can affect electron-phonon thermalization by decreasing the amount of energy in the electron system during electron-electron relaxation processes.

4 Conclusions

In nanodevices, ballistic transport of hot energy carriers can play a significant role in thermal processes. In this work, the effects of ballistic transport and subsequent electron cooling after short-pulsed laser heating are studied. The equation of electron energy transfer is established from the electron Boltzmann transport equation. The ballistic and diffusive contributions to electron thermal transport are studied by applying the ballistic-diffusive approximation to the EEET. In this development, electron-interface scattering is treated with the ballistic-diffusive approximation to the BTE, and the diffusive processes are assumed as electron-phonon scattering. The power transferred from the electron system during ballistic transport due to inelastic interface scattering can be over an order of magnitude greater than the diffusive component at high electron temperatures (4000 K). The temperature trends and values of ballistic to diffusive power transfer agree very well with previous experiments.

Acknowledgment

The authors gratefully acknowledge financial support from the Office of Naval Research MURI program, Grant No. N00014-07-1-0723. P.H. also gratefully acknowledges support from the NSF Graduate Student Research Program. The authors would like to thank Rich Salaway, Jennifer Simmons, John Duda, Justin Smoyer, and Mike Fish for insightful discussions.

Nomenclature

C = heat capacity, J m^{-3} K^{-1}
$D(\varepsilon)$ = electron density of states per unit energy, m^{-3} J^{-1}
d = film thickness, m
E = electric field, V m^{-1}
e = fundamental electric charge, C
F = Lorentz force, N
f = nonequilibrium electron statistical distribution function
f_0 = Fermi–Dirac distribution function
G = electron-phonon coupling factor, W m^{-3} K^{-1}
$\hbar$ = Planck's constant divided by 2π, J s
J = incident laser fluence, J m^{-2}
m = mass of an electron, kg
n = conduction electron number density, m^{-3}
P = power density, W m^{-3}
R = optical reflectivity
S = source term describing volumetric power absorbed from laser pulse, W m^{-3}
T = temperature, K
t = time, s
t_p = pulse width, s
U = electron energy density, J m^{-3}
v = electron velocity, m s^{-1}

Greek Symbols

δ = ballistic penetration depth, m
ε = electron energy, J
ε_F = Fermi energy, J
γ = linear coefficient to electronic heat capacity (Sommerfeld constant), J m^{-3} K^{-2}
τ = thermalization or relaxation time, s

Subscripts

0 = equilibrium
avg = time averaged
d = contribution from electrons traveling ballistically
c = collision
e = electron
ei = electron-interface
ep = electron-phonon
L = lattice
m = contribution from electron traveling diffusively in the medium
r = position
v = velocity
z = z direction

Appendix

Beginning with the familiar expression for the Fermi energy given (Chap. 6, Eq. (17) in Ref. [37])

$$\varepsilon_F = \frac{\hbar^2}{2m}(3\pi^2 n)^{2/3} \tag{A1}$$

where $\hbar$ is Planck's constant divided by 2π, and recognizing that the density of states per unit energy per unit volume, assuming a parabolic conduction band, is given by (Chap. 6, Eq. (20) in Ref. [37])

$$D(\varepsilon) = \frac{1}{2\pi^2}\left(\frac{2m}{\hbar^2}\right)^{3/2}\varepsilon^{1/2} \tag{A2}$$

Equation (A1) can be rearranged and inserted into Eq. (A2) to give

$$D(\varepsilon) = \frac{3n}{2}\left(\frac{\varepsilon}{\varepsilon_F}\right)^{1/2}\frac{1}{\varepsilon_F} \tag{A3}$$

which is the expression for the electron density of states per unit energy per unit volume used in the calculations in this work.

References

[1] Ivanov, D. S., and Zhigilei, L. V., 2003, "Combined Atomistic-Continuum Modeling of Short-Pulse Laser Melting and Disintegration of Metal Films," Phys. Rev. B, **68**, p. 064114.
[2] Wellershoff, S.-S., Hohlfeld, J., Gudde, J., and Matthias, E., 1999, "The Role of Electron-Phonon Coupling in Femtosecond Laser Damage of Metals," Appl. Phys. A: Mater. Sci. Process., **69**, pp. S99–S107.
[3] Wellershoff, S.-S., Gudde, J., Hohlfeld, J., Muller, J. G., and Matthias, E., 1998, "The Role of Electron-Phonon Coupling in Femtosecond Laser Damage of Metals," Proc. SPIE, **3343**, pp. 378–387.
[4] Beaurepaire, E., Merle, J.-C., Daunois, A., and Bigot, J.-Y., 1996, "Ultrafast Spin Dynamics in Ferromagnetic Nickel," Phys. Rev. Lett., **76**, pp. 4250–4253.
[5] Guidoni, L., Beaurepaire, E., and Bigot, J.-Y., 2002, "Magneto-Optics in the Ultrafast Regime: Thermalization of Spin Populations in Ferromagnetic Films," Phys. Rev. Lett., **89**, p. 017401.
[6] Hohlfeld, J., Matthias, E., Knorren, R., and Bennemann, K. H., 1997, "Nonequilibrium Magnetization Dynamics of Nickel," Phys. Rev. Lett., **78**, pp.

4861–4864.
[7] Koopmans, B., Van Kampen, M., Kohlhepp, J. T., and De Jonge, W. J. M., 2000, "Femtosecond Spin Dynamics of Epitaxial Cu(111)/Ni/Cu Wedges," Appl. Phys. Lett., **87**, pp. 5070–5072.
[8] van Kampen, M., Kohlhepp, J. T., de Jonge, W. J. M., Koopmans, B., and Coehoorn, R., 2005, "Sub-Picosecond Electron and Phonon Dynamics in Nickel," J. Phys.: Condens. Matter, **17**, pp. 6823–6834.
[9] Fann, W. S., Storz, R., Tom, H. W. K., and Bokor, J., 1992, "Direct Measurement of Nonequilibrium Electron-Energy Distributions in Subpicosecond Laser-Heated Gold Films," Phys. Rev. Lett., **68**, pp. 2834–2837.
[10] Del Fatti, N., Voisin, C., Achermann, M., Tzortzakis, S., Christofilos, D., and Vallee, F., 2000, "Nonequilibrium Electron Dynamics in Noble Metals," Phys. Rev. B, **61**, pp. 16956–16966.
[11] Sun, C. K., Vallee, F., Acioli, L., Ippen, E. P., and Fujimoto, J. G., 1993, "Femtosecond Investigation of Electron Thermalization in Gold," Phys. Rev. B, **48**, pp. 12365–12368.
[12] Sun, C. K., Vallee, F., Acioli, L., Ippen, E. P., and Fujimoto, J. G., 1994, "Femtosecond-Tunable Measurement of Electron Thermalization in Gold," Phys. Rev. B, **50**, pp. 15337–15348.
[13] Hohlfeld, J., Wellershoff, S.-S., Gudde, J., Conrad, U., Jahnke, V., and Matthias, E., 2000, "Electron and Lattice Dynamics Following Optical Excitation of Metals," Chem. Phys., **251**, pp. 237–258.
[14] Hopkins, P. E., and Norris, P. M., 2007, "Substrate Influence in Electron-Phonon Coupling Measurements in Thin Au Films," Appl. Surf. Sci., **253**, pp. 6289–6294.
[15] Hostetler, J. L., Smith, A. N., Czajkowsky, D. M., and Norris, P. M., 1999, "Measurement of the Electron-Phonon Coupling Factor Dependence on Film Thickness and Grain Size in Au, Cr, and Al," Appl. Opt., **38**, pp. 3614–3620.
[16] Qiu, T. Q., Juhasz, T., Suarez, C., Bron, W. E., and Tien, C. L., 1994, "Femtosecond Laser Heating of Multi-Layer Metals—II. Experiments," Int. J. Heat Mass Transfer, **37**, pp. 2799–2808.
[17] Qiu, T. Q., and Tien, C. L., 1994, "Femtosecond Laser Heating of Multi-Layer Metals—I. Analysis," Int. J. Heat Mass Transfer, **37**, pp. 2789–2797.
[18] Klopf, J. M., and Norris, P. M., 2005, "Subpicosecond Observation of Photoexcited Carrier Thermalization and Relaxation in InP-Based Films," Int. J. Thermophys., **26**, pp. 127–140.
[19] Klopf, J. M., and Norris, P. M., 2007, "Probing Nonequilibrium Dynamics With White Light Femtosecond Pulses," Appl. Surf. Sci., **253**, pp. 6305–6309.
[20] Norris, P. M., Caffrey, A. P., Stevens, R. J., Klopf, J. M., Mcleskey, J. T., and Smith, A. N., 2003, "Femtosecond Pump-Probe Nondestructive Examination of Materials," Rev. Sci. Instrum., **74**, pp. 400–406.
[21] Chen, J. K., Latham, W. P., and Beraun, J. E., 2005, "The Role of Electron-Phonon Coupling in Ultrafast Laser Heating," J. Laser Appl., **17**, pp. 63–68.
[22] Brorson, S. D., Fujimoto, J. G., and Ippen, E. P., 1987, "Femtosecond Electronic Heat-Transport Dynamics in Thin Gold Films," Phys. Rev. Lett., **59**, pp. 1962–1965.
[23] Hohlfeld, J., Muller, J. G., Wellershoff, S.-S., and Matthias, E., 1997, "Time-Resolved Thermoreflectivity of Thin Gold Films and Its Dependence on Film Thickness," Appl. Phys. B: Lasers Opt., **64**, pp. 387–390.
[24] Chen, G., 2002, "Ballistic-Diffusive Equations for Transient Heat Conduction From Nano to Macroscales," ASME J. Heat Transfer, **124**, pp. 320–328.
[25] Chen, G., 2001, "Ballistic-Diffuse Heat-Conduction Equations," Phys. Rev. Lett., **86**, pp. 2297–2300.
[26] Vincenti, W. G., and Kruger, C. H., 2002, *Introduction to Physical Gas Dynamics*, Krieger, Malabar, FL.
[27] Kaganov, M. I., Lifshitz, I. M., and Tanatarov, L. V., 1957, "Relaxation Between Electrons and the Crystalline Lattice," Sov. Phys. JETP, **4**, pp. 173–178.
[28] Smith, A. N., Hostetler, J. L., and Norris, P. M., 1999, "Nonequilibrium Heating in Metal Films: An Analytical and Numerical Analysis," Numer. Heat Transfer, Part A, **35**, pp. 859–873.
[29] Chen, J. K., Tzou, D. Y., and Beraun, J. E., 2006, "A Semiclassical Two-Temperature Model for Ultrafast Laser Heating," Int. J. Heat Mass Transfer, **49**, pp. 307–316.
[30] Swartz, E. T., and Pohl, R. O., 1989, "Thermal Boundary Resistance," Rev. Mod. Phys., **61**, pp. 605–668.
[31] Qiu, T. Q., and Tien, C. L., 1993, "Heat Transfer Mechanisms During Short-Pulse Laser Heating of Metals," ASME J. Heat Transfer, **115**, pp. 835–841.
[32] Yang, R., Chen, G., Laroche, M., and Taur, Y., 2005, "Simulation of Nanoscale Multidimensional Transient Heat Conduction Problems Using Ballistic-Diffusive Equations and Phonon Boltzmann Equation," ASME J. Heat Transfer, **127**, pp. 298–306.
[33] Majumdar, A., 1993, "Microscale Heat Conduction in Dielectric Thin Films," ASME J. Heat Transfer, **115**, pp. 7–16.
[34] Lin, Z., Zhigilei, L. V., and Celli, V., 2008, "Electron-Phonon Coupling and Electron Heat Capacity of Metals Under Conditions of Strong Electron-Phonon Nonequilibrium," Phys. Rev. B, **77**, p. 075133.
[35] Chen, G., 2005, *Nanoscale Energy Transport and Conversion: A Parallel Treatment of Electrons, Molecules, Phonons, and Photons*, Oxford University Press, New York.
[36] Chowdhury, I. H., and Xu, X., 2003, "Heat Transfer in Femtosecond Laser Processing of Metal," Numer. Heat Transfer, Part A, **44**, pp. 219–232.
[37] Kittel, C., 1996, *Introduction to Solid State Physics*, Wiley, New York.
[38] Qiu, T. Q., and Tien, C. L., 1992, "Short-Pulse Laser Heating on Metals," Int. J. Heat Mass Transfer, **35**, pp. 719–726.
[39] Smith, A. N., and Norris, P. M., 1998, "Numerical Solution for the Diffusion of High Intensity, Ultrashort Laser Pulses Within Metal Films," *Proceedings of the 11th International Heat Transfer Conference (Korean Society of Mechanical Engineers)*, Vol. 5, p. 241–246.
[40] Hostetler, J. L., Smith, A. N., and Norris, P. M., 1997, "Thin-Film Thermal Conductivity and Thickness Measurements Using Picosecond Ultrasonics," Microscale Thermophys. Eng., **1**, pp. 237–244.
[41] Smith, A. N., and Norris, P. M., 2001, "Influence of Intraband Transitions on the Electron Thermoreflectance Response of Metals," Appl. Phys. Lett., **78**, pp. 1240–1242.